

**Tetraspanin dependent tunneling nanotubule formation mediates stromal and cancer cell interactions and facilitates ovarian cancer metastasis**

by

**Julia Kooser**

Microbiology, University of Pittsburgh, 2021

Submitted to the Graduate Faculty of the  
University Honors College in partial fulfillment  
of the requirements for the degree of  
Bachelor of Philosophy

University of Pittsburgh

2021

UNIVERSITY OF PITTSBURGH

UNIVERSITY HONORS COLLEGE

This thesis was presented

by

**Julia Kooser**

It was defended on

March 24, 2021

and approved by

Valerie Oke, Assistant Chair, Department of Biological Sciences

Stefanie Hedayati, Lecturer, Department of Biological Sciences

Karen Mclean, Assistant Professor, Department of Gynecologic Oncology, University of

Michigan

Thesis Advisor/Dissertation Director: Lan Coffman, Assistant Professor, Department of

Medicine

Copyright © by Julia Kooser

2021

# **Tetraspanin dependent tunneling nanotubule formation mediates stromal and cancer cell interactions, and facilitates ovarian cancer metastasis**

Julia Kooser, BPhil

University of Pittsburgh, 2021

Ovarian cancer is the most fatal gynecological cancer in the United States, due to the propensity for early metastasis. Tumor cells do not grow in isolation but reside within a complex environment termed the tumor microenvironment. Mesenchymal stem cells, which are multipotent stromal progenitor cells found within most tissues of the body, can support a pro-tumorigenic environment, especially when they are epigenetically reprogrammed to assume a cancer associated phenotype referred to as cancer-associated mesenchymal stem cells.

Our lab has shown that cancer-associated mesenchymal stem cells interact directly with tumor cells to promote metastasis of ovarian cancer. More specifically, our lab has shown that tetraspanins, (CD9, CD151, CD63, CD81) proteins with transmembrane domains and highly expressed on the surface of cells, may mediate these direct interactions. Based on these findings, it is hypothesized tetraspanins mediate direct interactions between tumor cells and cancer-associated mesenchymal stem cells to increase metastatic potential of ovarian cancer. To assess localization of tetraspanins in relation to tumor cells and cancer-associated mesenchymal stem cell, and to determine proximity of tetraspanins at cell contact points, a co-immunofluorescence (co-IF) staining and proximity ligation assay (PLA) was performed. Then, co-immunoprecipitation (co-IP) experiments were performed for further investigation of protein-protein interactions between tetraspanins.

The co-IF showed that cancer-associated mesenchymal stem cells express CD81 and CD63 while tumor cells mostly express CD9. Next, the PLA showed that (CD9-CD63) and (CD9-CD81) are in proximity at tumor cell and cancer-associated mesenchymal stem cell junctions. Further, CD63 and CD81 were detected after precipitating CD9 using the coIP. Taken together, these results indicate that CD9 directly binds to CD63 and CD81. Since direct interactions between cancer-associated mesenchymal stem cells and ovarian cancer cells are implicated in ovarian cancer metastasis, and these tetraspanins were shown to be upregulated on the surface of cancer-associated mesenchymal stem cells and tumor cells, tetraspanins may act as a causal agent in promoting lethality and metastasis of ovarian cancer.

## Table of Contents

<b>Preface.....</b>	<b>x</b>
<b>1.0 Introduction.....</b>	<b>1</b>
<b>2.0 Materials and Methods.....</b>	<b>7</b>
<b>2.1 Cell Culture.....</b>	<b>7</b>
<b>2.2 Identification of mesenchymal stem cells .....</b>	<b>7</b>
<b>2.3 RNA extraction .....</b>	<b>8</b>
<b>2.4 cDNA synthesis .....</b>	<b>9</b>
<b>2.5 Characterization of cancer-associated mesenchymal stem cells .....</b>	<b>9</b>
<b>2.6 Immunofluorescent staining of cancer-associated mesenchymal stem cell and tumor         cell interactions.....</b>	<b>10</b>
<b>2.7 Proximity Ligation Assay (PLA) for tetraspanin associations.....</b>	<b>11</b>
<b>2.8 Co-immunoprecipitation assessing binding of CD9 to CD63 and CD81.....</b>	<b>12</b>
<b>3.0 Results .....</b>	<b>14</b>
<b>3.1 Classification of cancer-associated mesenchymal stem cells .....</b>	<b>14</b>
<b>3.2 CD9 is present on tumor cells at cancer-associated mesenchymal stem cell and tumor         cell junctions, while CD63 and CD81 are present on cancer-associated         mesenchymal stem cells at cell junctions.....</b>	<b>14</b>
<b>3.3 CD9, CD63, and CD81 are in very close proximity to each other at cancer-associated         mesenchymal stem cell and tumor cell junctions, implicating them in direct         interactions.....</b>	<b>17</b>

<b>3.4 Co-Immunoprecipitation indicates (co-IP) indicates that CD9, 63, and 81 directly interact.....</b>	<b>19</b>
<b>3.5 As determined by immunofluorescent staining, mitochondria and f-actin are present at cancer-associated mesenchymal stem cell and tumor cell junctions .....</b>	<b>21</b>
<b>4.0 Discussion.....</b>	<b>23</b>
<b>Bibliography .....</b>	<b>27</b>

## List of Tables

<b>Table 1: Classification of cancer association of patient's tissue .....</b>	<b>15</b>
--	-----------



## List of Figures

<b>Figure 1: Flowcytometry screen identified that CD9 and CD151 are abundant on cancer cell surface and CD63 and CD81 are abundant on the cancer associated mesenchymal stem cell surface (CA-MSCs).</b> .....	<b>6</b>
<b>Figure 2: CD9 and CD63 interact at cancer-associated mesenchymal stem cell and tumor cell contact points as assessed via co-immunofluorescence.</b> .....	<b>16</b>
<b>Figure 3: CD9 is in very close proximity to CD63 and CD81 at cancer-associated mesenchymal stem cell and tumor cell contact points.</b> .....	<b>18</b>
<b>Figure 4: Co-IP assessed binding of CD63 and CD81 to CD9 in cocultured cancer-associated mesenchymal stem cells and tumor cells.</b> .....	<b>20</b>
<b>Figure 5: Mitochondria and f-actin localization in cocultured cancer-associated mesenchymal stem cell and tumor cells.</b> .....	<b>22</b>
<b>Figure 6: CD9 heterodimerizes with CD63 and CD81 to potentially facilitate tunneling nanotubule formation and mitochondrial transfer to increase metastatic potential of ovarian cancer.</b> .....	<b>26</b>

## **Preface**

I would like to thank Dr. Lan Coffman for overseeing this project as the Principal Investigator. In addition, I would also like to thank Dr. Huda Atiya for providing oversight as a post-doctoral fellow. I would like to thank Dr. Lan Coffman for functioning as my thesis advisor. I would also like to thank Dr. Valerie Oke, Dr. Stefanie Hedayati, and Dr. Karen Mclean for serving on my thesis committee. Finally, I would like to thank the Magee Women's Research Institute for providing funding for this project.

## 1.0 Introduction

Ovarian cancer is the most fatal gynecological cancer in the United States due to early metastasis (Ghoneum, Afify, Salih, Kelly, & Said, 2018). Over 70% of ovarian cancer cases are diagnosed at late stages, resulting in a 30% 5-year survival rate (Yeung et al., 2015). Epithelial ovarian cancer is a heterogeneous disease which includes multiple histological subtypes including endometrioid, clear cell and mucinous histologies. However, high grade serous ovarian cancer (HGSOC) is the most common epithelial ovarian cancer<sup>1</sup>. Despite heterogeneity in cancer subtypes, all ovarian cancer cells preferentially metastasize to the peritoneal cavity (Ghoneum et al., 2018). This rapid metastasis accounts for the high lethality of ovarian cancer. Since metastasis is the source of increased mortality, understanding its biological underpinnings may provide insight into reducing the pathogenicity of ovarian cancer.

There is complex molecular crosstalk between tumor cells and non-malignant connective tissue cells (Keating, 2006), termed stromal cells, in the tumor microenvironment, which contributes to the progression of ovarian cancer (Atiya, Frisbie, Pressimone, & Coffman, 2020). Mesenchymal stem cells are multipotent stromal cells and play an essential role in maintaining the tumor microenvironment (Atiya et al., 2020). They can differentiate into stromal cell types in the tumor microenvironment, such as adipocytes and fibroblasts, and also induce angiogenesis and modulate the immune response (Hass, 2020). Mesenchymal stem cells can be distinguished from other stromal or microenvironmental cells by distinct cell surface proteins, their strong plastic adherence, and their ability to differentiate into other stromal cells (Dominici et al., 2006). The International Society for Cellular Therapy has defined specific criteria that need to be met to identify a mesenchymal stem cell, including expression of CD105, CD73, CD90, and absence of

CD45, CD34, CD14 or CD11b, CD79 $\alpha$  or CD19 and HLA-DR surface molecules (Dominici et al., 2006).

Normal mesenchymal stem cells can undergo a change in epigenetic programming to become cancer-associated mesenchymal stem cells(Coffman et al., 2019). More specifically, tumor cells further increase the cancer association of mesenchymal stem cells by inducing DNA methylation changes, histone modifications, and alterations in chromosomal accessibility(Coffman et al., 2019). These epigenetic modifications cause differential transcription of specific genes, which subsequently enhances the metastatic potential of cancer-associated mesenchymal stem cells<sup>7</sup>. The unique transcriptomic profiles in mesenchymal stem cells were utilized to build a logistic regression model to distinguish normal mesenchymal stem cells from cancer-associated mesenchymal stem cells(Coffman et al., 2019). Relative to normal mesenchymal stem cells, cancer-associated mesenchymal stem cells have increased mRNA expression of ANXA8L2, GATA4, and TGF- $\beta$ (Coffman et al., 2019). Cancer-associated mesenchymal stem cells also showed reduced mRNA expression of COL15A1, CRLF1 and IRX2 compared to normal mesenchymal stem cells<sup>7</sup>. Cancer-associated mesenchymal stem cells are strongly pro-tumorigenic, creating a more chemotherapy resistant, hyperproliferative phenotype in ovarian cancer(Coffman et al., 2019). Mesenchymal stem cells have been implicated in tumor cell metastasis via paracrine signaling through cytokines, exosomes, metabolites and microvesicles (Melzer, Yang, & Hass, 2016). Mesenchymal stem cells also utilize direct interactions with tumor cells to increase metastasis via Notch signaling, synthesis of gap junctions, and nanotube formation(Melzer et al., 2016).

Because of the influence of cancer-associated mesenchymal stem cells in creating a more pathogenic phenotype in ovarian cancer, experiments were performed to characterize the

interactions between cancer-associated mesenchymal stem cells and tumor cells(Fan et al., 2020). Since direct interactions between tumor cells and cancer-associated mesenchymal stem cells have been implicated in epigenetic alterations in mesenchymal stem cells, it was hypothesized that direct interactions mediate metastasis and pathogenicity of ovarian cancer(Coffman et al., 2019). To determine if direct interactions are needed to increase metastatic potential of ovarian cancer, cancer-associated mesenchymal stem cells and tumor cells were co-cultured and injected into mice to assess the rate of metastasis (Fan et al., 2020). It was demonstrated that tumor cells cocultured with cancer-associated mesenchymal stem promote metastasis of ovarian cancer to the lungs and peritoneal cavity in mice (Fan et al., 2020). To determine if cancer-associated mesenchymal stem cells promote metastasis via direct or indirect interactions, cancer-associated mesenchymal stem cells were encapsulated into alginate, which immobilizes and physically separates cells. Alginate verified that direct, physical interactions, and not cell signaling, are needed for metastasis. To assess the ability of both encapsulated and non-encapsulated cancer-associated mesenchymal stem cells to signal in a paracrine manner to tumor cells, cancer-associated mesenchymal stem cells were transduced via lentivirus with a construct which makes the cells constitutively secrete luciferase. There was no difference in present of luciferase in media between encapsulated and non-encapsulated cancer-associated mesenchymal stem cells, verifying that encapsulation prevents the direct interaction between cancer-associated mesenchymal stem cells and tumor cells but allows for exchange of secreted factors<sup>9</sup>. This experiment was performed to determine if direct interactions between tumor cells and cancer-associated mesenchymal stem cells were needed to increase metastasis of ovarian cancer. Interestingly, when cancer-associated mesenchymal stem cells were encapsulated and grown with tumor cells in a mouse model, there was a significant reduction in metastasis<sup>9</sup>. These findings suggest that direct interactions between tumor cells and

cancer-associated mesenchymal stem cells are needed to increase the metastatic potential of ovarian cancer.

Due to the importance of direct cellular interactions driving ovarian cancer metastasis, the surface proteins that mediate the cancer-associated mesenchymal stem cell and tumor cell interactions were investigated (Goldfeld, Atiya, Frisbie, & Coffman, 2020). To determine which surface proteins mediate these direct interactions, a lyoplate flow cytometry screening panel (Goldfeld et al., 2020) was utilized to assess which surface proteins were differentially expressed on the surface of cancer-associated mesenchymal stem cells and tumor cells (**Figure 1**) (Goldfeld et al., 2020). Over 200 proteins established as being expressed on the surface of cells were included in the screening panel. The top 20 surface proteins identified on tumor cell and cancer-associated mesenchymal stem cells were utilized to narrow down the proteins implicated in direct interactions. The presence of the proteins on the surface of a different, independent set of tumor cells and cancer-associated mesenchymal stem cells was assessed using flow cytometry, RT-qPCR, and western blotting. Four proteins expressed at high abundance on the surface of tumor cells and cancer-associated mesenchymal stem cells were identified (Goldfeld et al., 2020). These four proteins were from the tetraspanin superfamily of proteins. More specifically, CD9 and CD151 had increased expression on tumor cells while CD63 and CD81 had increased surface expression on cancer-associated mesenchymal stem cells. Interestingly, these tetraspanins have previously been implicated in intercellular interactions in pancreatic cancer due to their presence on the surface of exosomes (Khushman et al., 2017). The flow cytometry screen suggests tetraspanins may mediate cancer-associated mesenchymal stem cell: tumor interactions to increase pathogenicity of ovarian cancer.

A literature review demonstrated evidence that CD9 may bind with both CD63 and CD81<sup>11</sup>. This raises the possibility that CD9 and CD151 on the surface of tumor cells may bind to CD63 and CD81 on the surface of cancer-associated mesenchymal stem cells.

Taking this information into consideration, it was determined that CD9 and CD63 and CD81 mediate direct interactions between cancer-associated mesenchymal stem cells and tumor cells. I also aim to elucidate the role of these proteins, and direct interactions in promoting ovarian cancer metastasis.

Donation of mitochondria from stromal cells to tumor cells has previously been implicated in cancer progression (Nocquet, Juin, & Souazé, 2020). Mitochondrial donation has been associated with pathogenic phenotypes in tumor cells, such as resistance to apoptosis, which is associated with a more hyperproliferative and pathogenic phenotype in ovarian cancer (Jackson et al., 2016). Tunneling nanotubules, membrane protrusions containing f-actin, have previously been implicated in mitochondrial transfer (Wang & Gerdes, 2015). More specifically, phagocytic activity, which is modulated by mitochondrial transfer, was greatly reduced in macrophages in which tunneling nanotubule formation was inhibited (Jackson et al., 2016). Mitochondrial transfer between stromal cells and cancer cells has previously been implicated in increased oxidative phosphorylation, ATP production, and increased proliferation in tumor cells (Herst, Dawson, & Berridge, 2018). However, the exact mechanism by which mitochondrial transfer contributes to pathogenicity remains unknown. Since mitochondrial transfer is a newly emerging area in cancer biology, I am interested in determining if cancer-associated mesenchymal stem cells utilize their direct interaction with tumor cells to donate mitochondria as a mechanism to increase ovarian cancer metastasis

I hypothesize that tetraspanins mediate direct interactions between cancer-associated mesenchymal stem and tumor cells by promoting tunneling nanotubule formation and subsequent mitochondrial transfer.

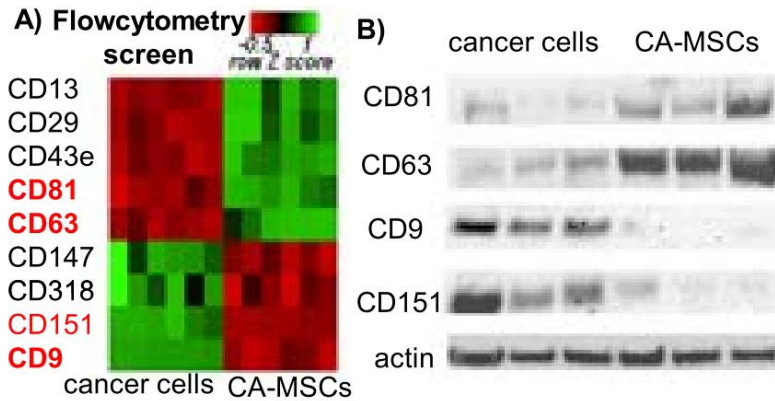


**Figure 1: Flowcytometry screen identified that CD9 and CD151 are abundant on cancer cell surface and CD63 and CD81 are abundant on the cancer associated mesenchymal stem cell surface (CA-MSCs). A) Proteins with highest surface expression on cancer cells and cancer-associated mesenchymal stem cells identified via lyoplate flow cytometry screen. Green represents increased surface expression of proteins. Red indicates decreased surface expression. B) Validation of flowcytometry screening results via western blot. Patient derived ascites cancer cells and cancer-associated mesenchymal stem cells were isolated, lysed and proteins probed with anti-CD81, CD-63, CD-9. CD151 and actin (as a loading control) <sup>10</sup>.**



## **2.0 Materials and Methods**

### **2.1 Cell Culture**

Primary cell lines from women with ovarian cancer were utilized through an active IRB tissue collection protocol. Tumor cell lines included high-grade serous cell lines OVSAHO and OVCAR3 and primary, patient-derived cell line pt412. Tumor cells were tested monthly for mycoplasma contamination and cultured in DMEM media supplemented with 10% heat activated fetal bovine serum (FBS) and 1% penicillin/streptomycin. OVSAHO and OVCAR3 cell lines were obtained through the American Type Culture Collection (ATCC). Cancer-associated mesenchymal stem cells were isolated from high grade serous tumor samples as previously described(Au - Atiya, Au - Orellana, Au - Wield, Au - Frisbie, & Au - Coffman, 2021). Cancer-associated mesenchymal stem cells were cultured in mammary epithelial cell basal medium (MEBM), supplemented with 10% heat-inactivated FBS, 1X B27, 20 ng/mL EGF, 1 ng/mL hydrocortisone, 5 µg/mL insulin, 100 µM β-mercaptoethanol, 10 ng/mL β-FGF, 1% penicillin/streptomycin, and 20 µg/mL gentamicin.

### **2.2 Identification of mesenchymal stem cells**

Mesenchymal stem cells were isolated so they could be cocultured with tumor cells. To identify mesenchymal stem cells, samples were sorted by flow cytometry for expression of CD90, CD105 and CD73(McLean et al., 2011). Previously established by the International Society of

Cell Therapy(McLean et al., 2011), mesenchymal stem cells must express CD105, CD73, CD90 and not express CD45, CD34, CD14 or CD11b, CD79 $\alpha$  or CD19 and HLA-DR. Isolated cells were more than 95% positive and negative for these markers. Once cells were established as having an appropriate marker profile, a differentiation assay was performed to ensure cells had multipotent properties consistent with mesenchymal stem cells. AS a part of this assay, the ability of mesenchymal stem cells to differentiate into fibroblasts, chondrocytes, adipocytes, and osteocytes was assessed as previously described (Au - Atiya et al., 2021). Mesenchymal stem cells were used at passage 8 or less to limit the potential for spontaneous differentiation or altered phenotype related to extensive in vitro tissue culture passage.

### **2.3 RNA extraction**

To isolate RNA for reverse transcriptase quantitative polymerase chain reaction (RT-qPCR), cells were lysed with Buffer RA1 and  $\beta$ -mercaptoethanol. 70% ethanol was then added to the lysate. This was mixed vigorously and then filtered through a NucleoSpin filter. Lysate was then added to a new collection tube and then 350  $\mu$ L Membrane Desalting Buffer was added to lysate to remove salt and optimize conditions for rDNase digestion. To inactivate rDNase, 200  $\mu$ Ls RAW2 was added to RNA Column and centrifuged. Next, the column was washed twice with buffer RA3 and RNA was eluted with 36  $\mu$ Ls RNase-free water.

## **2.4 cDNA synthesis**

Once the RNA extraction was completed, cDNA synthesis was performed. For this procedure, 8  $\mu\text{L}$  RNA from the sample were added to a PCR tube with 1  $\mu\text{L}$  dNTP mix and 1  $\mu\text{L}$  random hexamer primer. This solution was then incubated at 65 °C for 5 minutes and then placed on ice for 1 minute. Next, a master mix was prepared. This master mix contained 2  $\mu\text{L}$  10x RT buffer, 4  $\mu\text{L}$  25 mM  $\text{MgCl}_2$  and 2  $\mu\text{L}$  0.1 M DTT mix per reaction. After samples were removed from incubation, 9  $\mu\text{L}$  of this master mix was added to one sample that functioned as a negative control to ensure there was no amplification of genomic DNA that may be present after the RNA extraction. Next, 1  $\mu\text{L}$  per reaction of SuperScript III Reverse Transcriptase was added to master mix. 10  $\mu\text{L}$  per reaction of master mix was added to all remaining samples. These samples were then incubated for 50 °C for 50 minutes, 25 °C for 10 minutes, and then 50 °C for 50 minutes. After reaction, 1  $\mu\text{L}$  RNase H was added to each sample and they were further incubated for 20 minutes at 37 °C.

## **2.5 Characterization of cancer-associated mesenchymal stem cells**

Previous work established a distinct epigenetic profile of cancer-associated mesenchymal stem cells compared to normal mesenchymal stem cells (Cianfanelli, Monlezun, & Coulthurst, 2015). These profiles have been utilized to create an algorithm assessing the cancer-association of mesenchymal stem cells. Cancer association was based on the differential expression of genes in mesenchymal stem cells associated with ovarian cancer tumor cells *in vivo* (Goldfeld et al., 2020). The expression of six genes of interest was assessed via RT-qPCR. These genes of interest include

ANXA8L2, COL15A1, CRLF1, GATA4, IRX2 and TGF- $\beta$ . Cancer-associated mesenchymal stem cells were classified based on their expression levels of these genes via RT-qPCR. The equation to classify their cancer association is  $1 / (1 + 0.00622^{(\text{ANXA8 expression} - \text{GAPDH expression})} + (0.175026^{(\text{COL15 expression} - \text{GAPDH expression})} + (0.886027^{(\text{CRLF1 expression} - \text{GAPDH expression})} + (-0.34594^{(\text{GATA4 expression} - \text{GAPDH expression})} + (0.416952^{(\text{IRX2 expression} - \text{GAPDH expression})} + (-0.00824^{(\text{TGF-}\beta \text{ expression} - \text{GAPDH expression})} - 7.62691))$ . Values of 0.96 and greater are consistent with cancer-associated mesenchymal stem cells while values of less than 0.30 are consistent with normal mesenchymal stem cells (Coffman et al., 2019).

## **2.6 Immunofluorescent staining of cancer-associated mesenchymal stem cell and tumor cell interactions**

Tumor cells were stained with CellTrace Red and then plated with unstained cancer-associated mesenchymal stem cells in a 1:1 ratio for 24 hours. Cells were fixed in 4% paraformaldehyde for 10 minutes. Cells were then permeabilized in 0.2% TritonX100 for 10 minutes. Samples were blocked with Duolink Blocking Solution and incubated with primary antibody for 100 minutes. A sample was incubated with no primary antibody to function as a negative control for autofluorescence. Anti-CD9 FITC conjugated antibody was used to identify CD9. Anti-CD63 PerCP-Cy conjugated antibody was used to identify CD63 and CD151 was identified with anti-CD151 BV421 conjugated antibody. Cells were incubated with 8  $\mu$ l CD9 and CD151 antibody and 2.5  $\mu$ L CD63 antibody, all at a concentration of 5  $\mu$ g/mL, in 200  $\mu$ l diluent. Cells were also stained individually with each antibody (Anti-CD9-FITC or anti-CD63-PerCP-Cy or anti-CD151-BV421) to control for any alteration in fluorescent signal due to co-stain with

multiple fluorescent antibodies (one antibody may potentially interfere with the binding of a different antibody). Images were taken with a confocal microscope.

## **2.7 Proximity Ligation Assay (PLA) for tetraspanin associations**

Tumor cells and cancer-associated mesenchymal stem cells were co-cultured for 24 hours on a glass coverslip. Cancer-associated mesenchymal stem cells and tumor cells were differentially fluorescently labeled to enable identification of each cell type. Cancer-associated mesenchymal stem cells were previously transduced with a Cox8-GFP lentiviral construct which labels all mitochondria green. Tumor cells were labeled with CellTrace Violet following manufacture protocol, using 5 $\mu$ M incubation for 30 minutes. After cells were cocultured, they were fixed and permeabilized in the same manner as cells utilized for immunofluorescence staining. Cells were incubated with CD9 and CD63 antibodies or CD9 and CD81 antibodies. Each antibody came from different animals with mouse derived anti-CD9, goat derived anti-CD63, and goat derived anti-CD81. This allowed for secondary antibodies to recognize only one of the pairs of primary antibodies used. Each secondary antibody was coupled to oligonucleotides bound to the primary antibodies. For CD9 and CD63 PLA, mouse anti-CD9 and goat anti-CD63 primary antibodies were added. Then rabbit anti-mouse secondary antibody with one half of the oligonucleotide probe and rabbit anti-goat secondary antibody with the other half of the oligonucleotide probe was added. The same procedure was performed for the CD9 and CD81 PLA but using mouse anti-CD9 and goat anti-CD81 primary antibodies. If proteins are within 40 nanometers of each other, the probes on each secondary antibody hybridize, which leads to rolling DNA synthesis (Bagchi, Fredriksson, & Wallén-Mackenzie, 2015). During rolling DNA synthesis, oligos coupled to fluorochromes bind

to the DNA, which creates a red fluorescent signal(Bagchi et al., 2015). To function as a negative control, two samples were prepared. One sample was only incubated with anti-CD9 primary antibody only while the other was incubated with no primary antibodies.

## **2.8 Co-immunoprecipitation assessing binding of CD9 to CD63 and CD81**

To provide evidence that CD9 may heterodimerize with CD63 and CD81, a co-IP was performed. Tumor cells and cancer-associated mesenchymal stem cells were cocultured for three days and treated with 3,3'-Dithiobis(sulfosuccinimidylpropionate) (DTSSP) to promote crosslinking between cell surface proteins and then lysed. Anti-CD9 antibody was coupled to magnetic beads overnight at 37 degrees Celsius. The anti-CD9 coupled beads were added to the co-cultured cell lysate at 4 degrees Celsius for 20 minutes. Bead: -cell suspension was then washed three times with extraction buffer. Cross linking was then reversed with Dithiothreitol (DTT). Immunoprecipitation was resuspended in SDS buffer. Samples were run on a sodium dodecyl sulphate-polyacrylamide gel electrophoresis (SDS-PAGE) gel. Gels were transferred to a nitrocellulose membrane for western blotting. One blot was created for each target protein. Anti-CD9 was used to identify CD9 protein in the immunoprecipitate. Anti-CD63 was used to identify CD63 in the immunoprecipitate and anti-CD81 was used to identify CD81 in the immunoprecipitate. All blots were incubated with antibodies at a 1:500 concentration. As a control, IgG was also coupled to beads. Since protein binding to IgG was not expected, this served as a negative control. Also, the whole cell lysate without immunoprecipitation functioned as another control. As the whole cell lysate or “input” contains all proteins in the cell while the

immunoprecipitated “sample” should have led to specific binding of CD9 to the anti-CD9 bead, there should be significant enrichment of CD9 protein in the sample relative to the input.

## **3.0 Results**

### **3.1 Classification of cancer-associated mesenchymal stem cells**

To assess the effect of cancer-associated mesenchymal stem cells on tumor cell metastasis, the mesenchymal stem cells were first classified to determine their cancer association. Mesenchymal stem cells were isolated from ovarian cancer patient tissue and screened for cell surface markers and differentiation ability to meet criteria for mesenchymal stem cells as described above. The algorithm previously established in our lab was utilized to ensure the mesenchymal stem cells fit our classification of cancer-associated mesenchymal stem cells (Coffman et al., 2019) (**Table 1**). Cells with a classifier score of  $>0.96$  were considered cancer associated and were therefore used for experimentation.

### **3.2 CD9 is present on tumor cells at cancer-associated mesenchymal stem cell and tumor cell junctions, while CD63 and CD81 are present on cancer-associated mesenchymal stem cells at cell junctions**

Given that the tetraspanins were identified as potential binding partners, the localization of the tetraspanins in relation to tumor cells and cancer-associated mesenchymal stem cells was tested. To determine if the tetraspanins directly interact, an immunofluorescence stain was performed. Tumor cells and cancer-associated mesenchymal stem cells were cocultured for 24 hours on a coverslip at a 1:1 cellular ratio. Immunofluorescence staining was performed to



determine the location of CD9, CD151, CD63 and CD81 (**Figure 2**). Colocalization of CD9 and CD63 at cancer-associated mesenchymal stem cell and tumor cell junctions was demonstrated, Interestingly, CD151 did not show the same level of localization at cancer- associated mesenchymal and tumor cell junctions.

**Table 1: Classification of cancer association of patient’s tissue**

MSC	Classifier Score
BRCA ROV P2 20-515	1.00
20-591 FT2 P2	1.00
20-510 BRCA2 RFT	0.65
20-591 FT4 P2	1.00
19-8-21 LFT endo MSC	0.02
19-821 endo RFT MSC	1.00
20-616 ROV tumor	1.00
20-510 BRCA2 LFT	0.25
20-515 RFT BRCA2	0.35
20-0038 asc P4	1.00
20-0035 asc Pi	0.98
20-443 ROV HGS Tumor	1.00
2-20-251-LOV	0.94
3-20-251 ROV	1.00
20-289 LFT	0.93
20-354 RFT sorted BRCA1	0.97
20-289 RFT BRCA2	0.77
20-45 RFT class p53	0.97
20-303 LFT MSC RADIC?	0.85

**Classification score for mesenchymal stem cells. Mesenchymal stem cells were isolated from patients.**

**Classifier score is based on expression of 6 genes differentially expressed in mesenchymal stem cells associated with ovarian cancer. Mesenchymal stem cells with a classifier score of 0.96 or greater were utilized for experimentation assessing the influence of cancer-associated mesenchymal stem cells on tumor cell metastasis.**

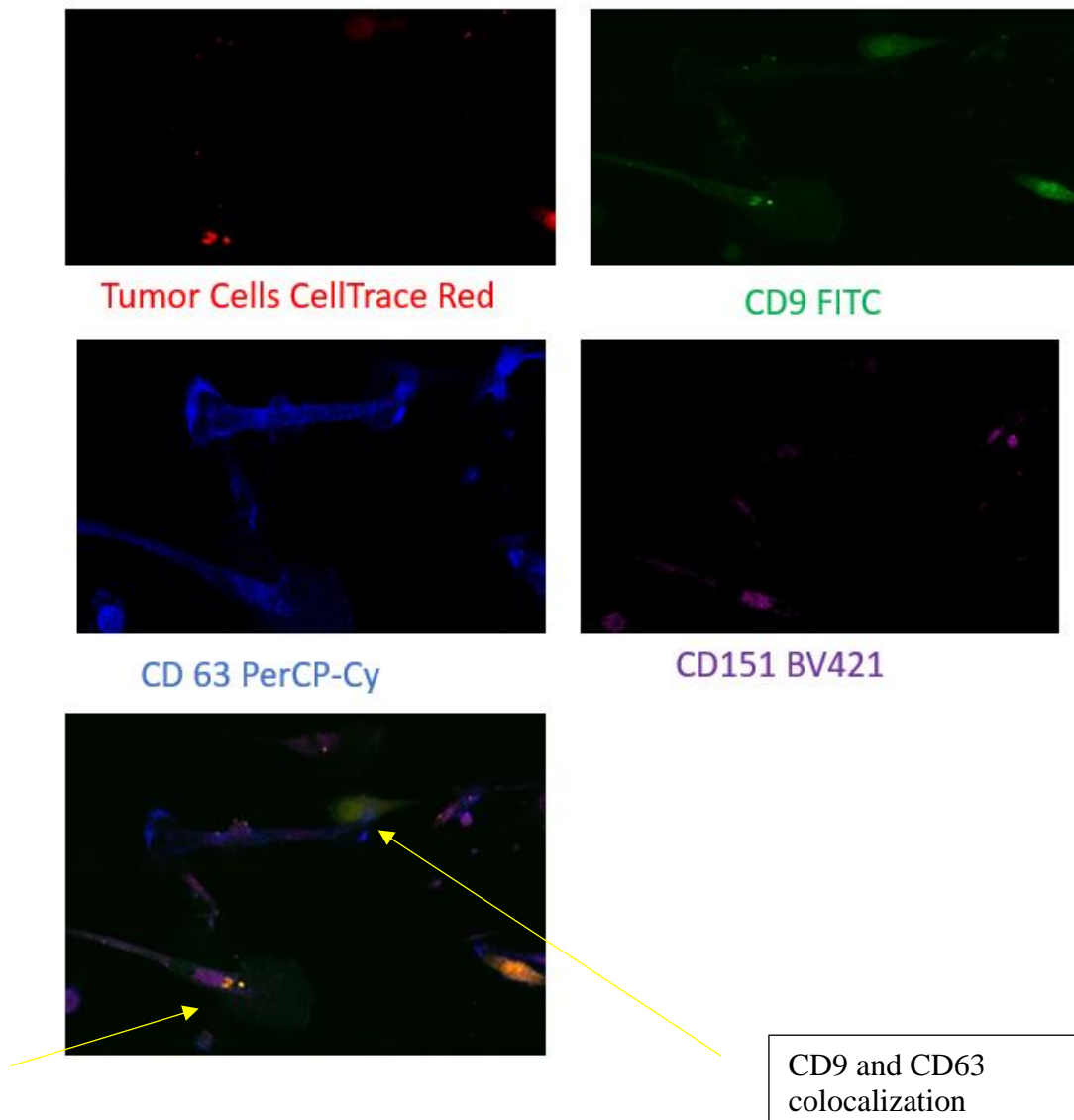
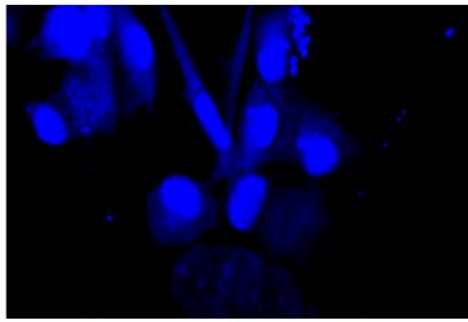


**Figure 2: CD9 and CD63 interact at cancer-associated mesenchymal stem cell and tumor cell contact points as assessed via co-immunofluorescence. Tumor cells were labeled with CellTrace Red. Cox8, a mitochondrial gene, was fused with GFP in cancer-associated mesenchymal stem cells (green). Tetraspanin CD63 was stained with PERCP-Cy (cyan). CD151 was stained with fluorochrome BV421 (violet). Images were overlaid to show localization of tetraspanins relative to tumor cells and cancer-associated mesenchymal stem cells. Arrows indicate colocalization of tetraspanins at tumor cells and cancer-associated mesenchymal stem cell contact points. Images were taken for two different tumor cell and cancer-associated mesenchymal stem cell lines. Of these lines, representative images were taken. This test was not performed on CD81 but will be during future experimentation.**

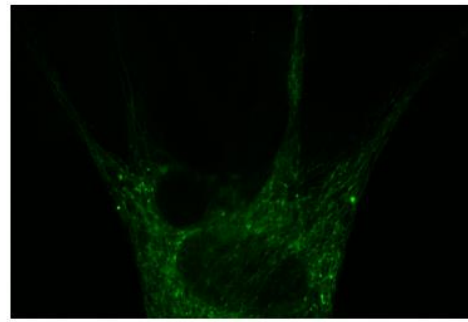
### **3.3 CD9, CD63, and CD81 are in very close proximity to each other at cancer-associated mesenchymal stem cell and tumor cell junctions, implicating them in direct interactions**

Given that immunofluorescence suggested CD9 and CD63 colocalize at cell contact points (**Figure 3**), I wanted to verify the proximity of these proteins to determine their role in cancer-associated mesenchymal stem cell and tumor cell binding. I utilized a proximity ligation assay, which enabled the determination of proteins in proximity. If proteins were within 40nm, probes on the secondary antibody localized to the proteins in proximity, which enabled DNA synthesis and fluorescent signal emission. During rolling DNA synthesis, oligos coupled to fluorochromes bound to the DNA synthesized, which resulted in fluorescent signal (Bagchi et al., 2015). The PLA was performed targeting CD9 and CD63, and CD9 and CD81. A PLA was not performed with CD151 due to the absence of localization at tumor cell and cancer-associated mesenchymal stem cell contact points. As shown in Figure 4, results demonstrated a fluorescent signal at cancer-associated mesenchymal stem cell: tumor cell junctions indicating CD9 and CD63 were in proximity at areas of cellular interaction. The results also indicated CD9 and CD81 were close to each other at cell contact points. These findings suggest that tetraspanins are involved in direct cancer-associated mesenchymal stem cell and tumor cell interactions and may facilitate direct interactions implicated in ovarian cancer metastasis.

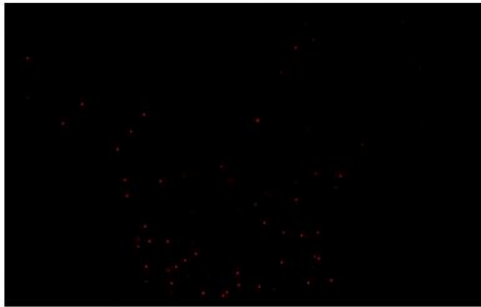
**A**



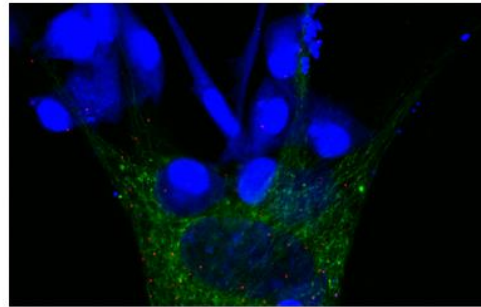
Tumor cells CellTrace Violet



CAMSCs GFP

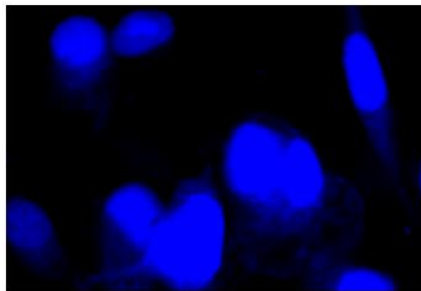


CD9 and CD63

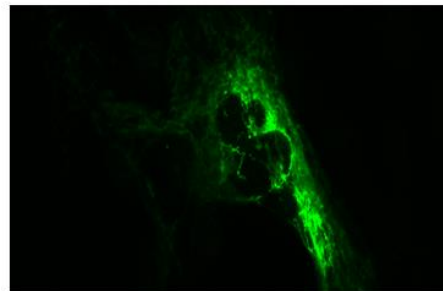


Merge

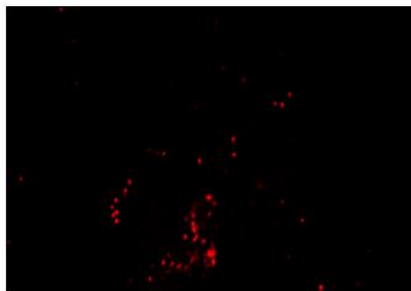
**B**



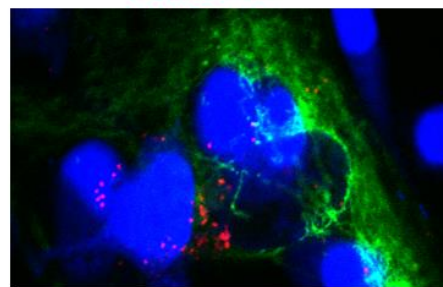
Tumor Cells CellTrace Violet



CAMSCs GFP



CD9 and CD81



Merge

**Figure 3: CD9 is in very close proximity to CD63 and CD81 at cancer-associated mesenchymal stem cell and tumor cell contact points A) Proximity ligation assay (PLA) assessing closeness of CD9 and CD63. CD9 and**

CD63 emit a signal at cancer-associated mesenchymal stem cell and tumor cell contact points (red), indicating these tetraspanins play a role in direct interactions. B) PLA assessing closeness of CD9 and CD81 (red) in cocultured cancer-associated mesenchymal stem cells and tumor cells. Tumor cells were labeled with CellTrace Violet (blue) while mitochondria of cancer-associated mesenchymal stem cells were labeled with GFP via COX8 fusion (green). Experiments were performed twice, and PLA signaling was observed at cell contact points both times.

### 3.4 Co-Immunoprecipitation indicates (co-IP) indicates that CD9, 63, and 81 directly interact

Given the confirmed proximity of CD9 with CD63 and CD81 using co-immunofluorescence and PLA, the lab next sought to identify direct protein- protein interactions occurring between the tetraspanins. Tumor cells were co-cultured with cancer-associated mesenchymal stem cells. These proteins were then crosslinked to maintain surface protein interactions. Co-cultured cells were harvested and lysed and a co-IP using anti-CD9 antibody for the immunoprecipitation step was performed. The whole cell lysate was used to assess if protein can be detected in the starting material prior to immunoprecipitation. If CD9 bound to the antibody coupled beads in the anti-CD9 immunoprecipitation, there should be significant enrichment of CD9 protein in the immunoprecipitation compared to the whole cell lysate. The first western panel was incubated with anti-CD9 antibody to ensure CD9 proteins were pulled down. In the second panel, the blot was incubated with anti-CD63 antibody to assess ability of CD63 to bind to CD9 and be co-immunoprecipitated. Finally, in the third panel, the blot was incubated with anti-CD81 to assess if CD81 was also co-immunoprecipitated with CD9. A western blot indicated CD81 and CD63 were co-immunoprecipitated along with CD9 (**Figure 4**). There was robust signal

indicating CD81 and CD63 bound to CD9. This preliminary data further implicated CD81, CD63 and CD9 in mediating direct interactions between cells.

There was also signal in the IgG immunoprecipitate, indicating there may have been nonspecific binding. Also, the sample signal was not at the expected 25 kDa size (the anticipated size of CD9, CD63 and CD81). To optimize protein interactions, proteins were crosslinked before cells were lysed and immunoprecipitated. However, the reversal of the crosslinking may have been unsuccessful, resulting in proteins remaining in complex and migrating on the gel at a larger than anticipated molecular weight. Also, there may have been non-specific binding of the antibodies with the western blot.

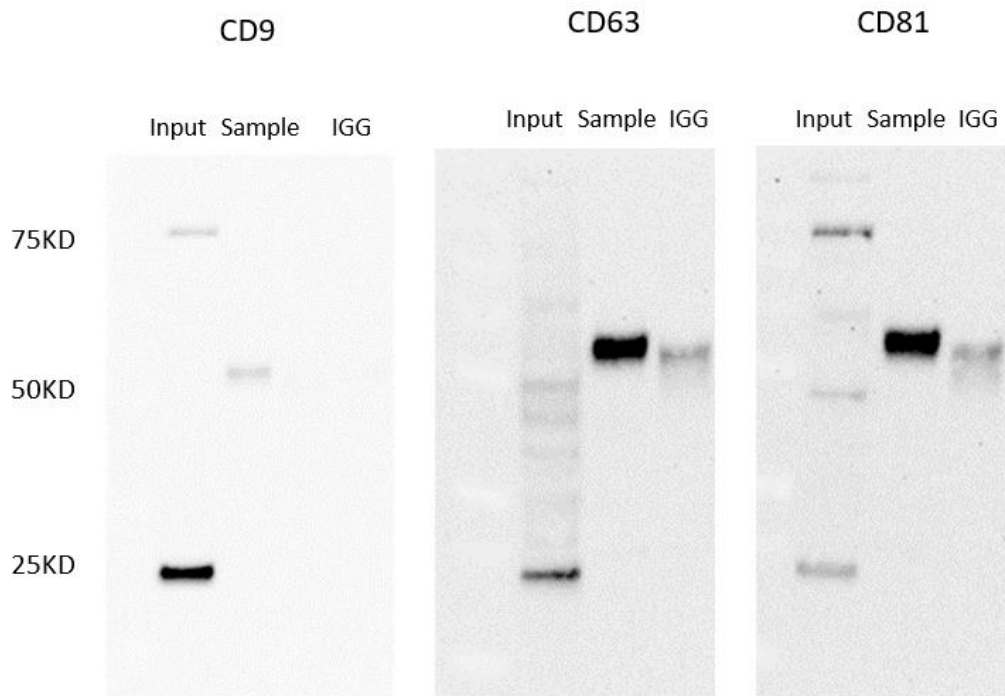


**Figure 4: Co-IP assessed binding of CD63 and CD81 to CD9 in cocultured cancer-associated mesenchymal stem cells and tumor cells. Cancer-associated mesenchymal stem cells and tumor cells were cocultured and**

cross-linked. Cell lysate was incubated with anti-CD9 coupled magnetic beads. Western blots were probed with either CD9, CD63 or CD81 antibodies. First panel assessed ability of CD9 to couple to magnetic beads. Second and third panel assessed binding of CD63 and CD81 to CD9, respectively. Whole cell lysate prior to immunoprecipitation functioned as a control while sample contained immunoprecipitated beads and complexed proteins. The positive signal for CD63 and CD81 in the sample lanes indicated co-precipitation of these tetraspanins with CD9. IgG was coupled to beads to function as a negative control. This was done once and will be repeated to optimize the results.

### **3.5 As determined by immunofluorescent staining, mitochondria and f-actin are present at cancer-associated mesenchymal stem cell and tumor cell junctions**

While performing experiments assessing direct interactions between tumor cells and cancer-associated mesenchymal stem cells, formation of f-actin containing projections between cells was observed. Since mitochondrial transfer to tumor cells has previously been implicated in facilitating tumor metastasis and has shown to be mediated by f-actin containing tunneling nanotubules, the role of tetraspanins in facilitating these interactions was explored (Herst et al., 2018; Wang & Gerdes, 2015).

Cancer-associated mesenchymal stem cells and tumor cells were cocultured in a 1:1 ratio for 24 hours and labeled mitochondria with RFP fused Cox8. F-actin was stained with phalloidin in cancer-associated mesenchymal stem cells since tunneling nanotubules have previously been implicated in direct interactions and organelle transfer. As shown in Figure 5, there was co-localization of mitochondrial and f-actin at stromal and tumor cell contact points. Based on these findings, it is hypothesized TNT formation at cancer-associated mesenchymal stem cell and tumor cell junctions may mediate direct interactions to increase mitochondrial transfer. While

tetraspanins have been implicated in direct cancer-associated mesenchymal stem cell and tumor cell interactions, the role of tetraspanins in facilitating TNT dependent mitochondrial transfer has not been investigated. Since tetraspanins are implicated in direct interactions between cancer-associated mesenchymal stem cells and tumor cells and tunneling nanotubule formation is an established consequence of these interactions, tetraspanins may facilitate intercellular TNT formation and mitochondrial transfer.

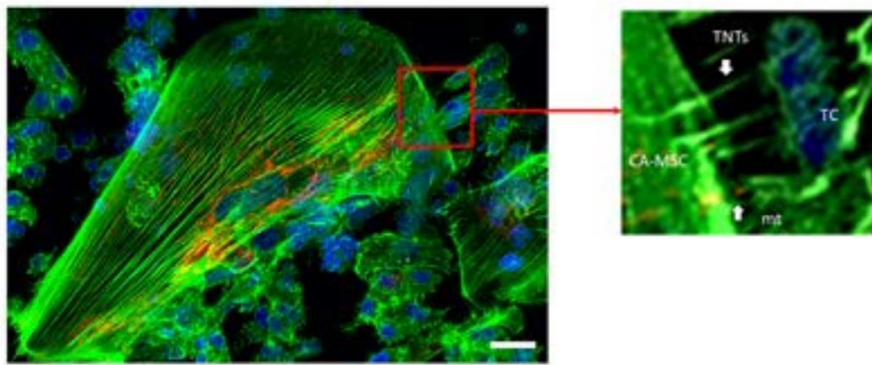


**Figure 5: Mitochondria and f-actin localization in cocultured cancer-associated mesenchymal stem cell and tumor cells. F-actin in cancer-associated mesenchymal stem cells was labeled with phalloidin (green). Mitochondria in cancer-associated mesenchymal stem cells were labeled with a RFP Cox8 fusion, and tumor cells were labeled with CellTrace Violet (blue). Images were taken via confocal microscopy. The insert shows localization of tunneling nanotubes (TNT) and mitochondria at cancer-associated mesenchymal stem cells and tumor cell junctions. Experiment was performed once and localization of mitochondria and tunneling nanotubules was observed.**



## 4.0 Discussion

It has been previously demonstrated that direct interactions between cancer-associated mesenchymal stem cells and tumor cells are necessary for ovarian cancer metastasis (Fan et al., 2020). Since previous findings have shown that these cancer-associated mesenchymal stem cell and tumor cell interactions are needed for tumor cell metastasis, understanding which proteins mediate this interaction provides insight into the essential role of cancer-associated mesenchymal stem cells in ovarian cancer metastasis.

Previous flow cytometry screening has shown tetraspanins CD9 and CD151 on tumor cells may potentially bind with CD63 and CD81 on cancer-associated mesenchymal stem cells (Goldfeld et al., 2020). Since these tetraspanins were highly expressed on the surface of cancer-associated mesenchymal stem cells and tumor cells and have previously been implicated in regulating progression of certain cancers<sup>11</sup>, the role of these tetraspanins in direct cell interactions was further investigated.

A co-IF was performed to assess localization of tetraspanins. The results show that tumor cells mostly express CD9 while CD63 and CD81 were expressed by cancer-associated mesenchymal stem cells. Since CD9 on tumor cells colocalized with CD63 and CD81 on cancer-associated mesenchymal stem cells, the co-IF results indicated that these tetraspanins may be involved in direct tumor cell and cancer-associated mesenchymal stem cell interactions.

Next, our PLA results show that these tetraspanins (CD9-CD63) and (CD9-CD81) are in proximity. Since the tetraspanins are in very close proximity, this provides further evidence the tetraspanins interact directly.

Our coIP results also support the hypothesis that CD9 and CD63 and CD81 mediate tumor cell to carcinoma associated mesenchymal stem cell binding. The coIP demonstrated CD81 and CD63 were pulled down during CD9 immunoprecipitation. These results suggest that proteins CD9 and CD63 and CD81 directly interact and may facilitate cellular binding. However, CD63 and CD81 were not detected at the expected molecular weight. This may be due to the proteins still being crosslinked, which will increase the apparent molecular weight. To address this, the coIP will be optimized to reverse the crosslinking. Also, there was reduced signal in the sample of the CD9 blot relative to the input. In the future, the coIP will be repeated with an increased concentration of anti-CD9 coupled to beads. Finally, there was signal when IgG antibody was coupled to beads. This indicates there was nonspecific binding. Due to this result, the coIP will be optimized with increased washing.

Collectively, these results support a critical role of CD9, CD63 and CD81 in mediating tumor cell to cancer-associated mesenchymal stem cell binding. In the future, our lab will create CRISPR-CAS9 CD9 knockout cancer cells to assess if CD9 is necessary and sufficient to allow binding between tumor cell and cancer-associated mesenchymal stem cells.

Since previous findings indicated that mitochondrial transfer is a consequence of direct cancer-associated mesenchymal stem cell and tumor cell interactions (Pressimone, Atiya, Frisbie, & Coffman, 2020), this process may be mediated by tetraspanins. More specifically, tunneling nanotubules are established as the primary means of intercellular mitochondrial transfer (Lu et al., 2017). Immunofluorescence staining of cocultured cancer-associated mesenchymal stem cells and tumor cells demonstrated that mitochondria and tunneling nanotubules are both present at cell junctions. To elucidate the role of tetraspanins in f-actin tunneling nanotubule formation, an experiment will be performed with CRISPR-CAS9 knockout of each tetraspanin (CD9 knockout

in tumor cells, CD81 and CD63 independently knocked out in cancer-associated mesenchymal stem cells). Tunneling nanotubule formation and mitochondrial transfer will then be assessed in i) CD9 knockout tumor cells grown with control cancer-associated mesenchymal stem cells, ii) control tumor cells with CD81 knockout cancer-associated mesenchymal stem cells, iii) control tumor cells with CD63 knockout cancer-associated mesenchymal stem cells and iv) control tumors cells with control cancer-associated mesenchymal stem cells.

For further investigation, specific knockout or antibody targeting experiments can be used to determine if these tetraspanins are implicated in cancer-associated mesenchymal stem cells-tumor cells binding, and subsequent metastasis.

Elucidating the role of tetraspanins in direct interactions may provide insight into how to mitigate metastasis, and ultimately lethality, of ovarian cancer. Prior to metastasis, ovarian cancer treatment can be managed with accessible, conventional therapeutic agents (Motohara et al., 2019). However, without clear symptoms and a hyperproliferative phenotype, ovarian cancer often goes undetected until it has preferentially metastasized throughout the peritoneum(Lengyel, 2010). Mouse models have shown that cancer-associated mesenchymal stem cells and tumor cells direct interactions are necessary for ovarian cancer metastasis<sup>9</sup>. If tetraspanins mediate stromal cell and tumor cell interactions to facilitate tunneling nanotubule formation and mitochondrial transfer to tumor cells, therapeutics reducing expression of these tetraspanins may be developed to reduce the rate of metastasis.

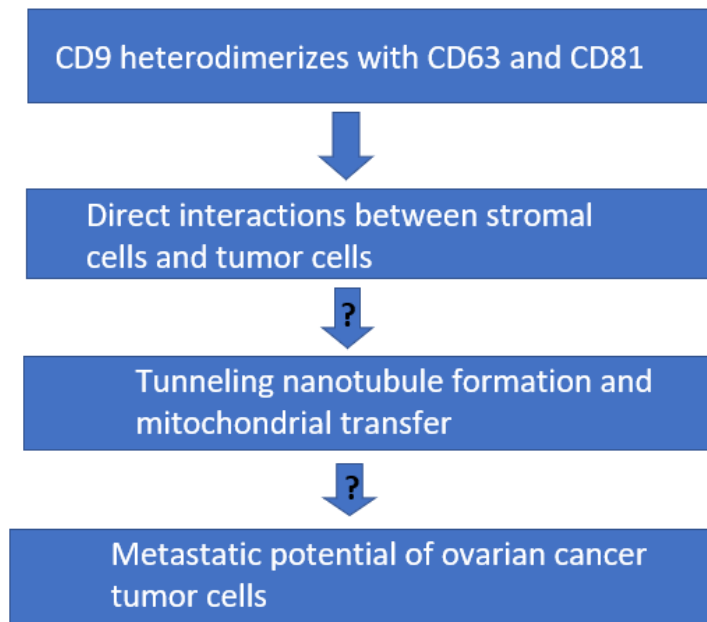


**Figure 6: CD9 heterodimerizes with CD63 and CD81 to potentially facilitate tunneling nanotubule formation and mitochondrial transfer to increase metastatic potential of ovarian cancer. This is a proposed schematic and will be tested with future experimentation.**

## Bibliography

1. Ghoneum, A., Afify, H., Salih, Z., Kelly, M. & Said, N. Role of tumor microenvironment in the pathobiology of ovarian cancer: Insights and therapeutic opportunities. *Cancer medicine* **7**, 5047-5056 (2018).
2. Yeung, T.L., *et al.* Cellular and molecular processes in ovarian cancer metastasis. A Review in the Theme: Cell and Molecular Processes in Cancer Metastasis. *American journal of physiology. Cell physiology* **309**, C444-456 (2015).
3. Keating, A. Mesenchymal stromal cells. *Curr Opin Hematol* **13**, 419-425 (2006).
4. Atiya, H., Frisbie, L., Pressimone, C. & Coffman, L. Mesenchymal Stem Cells in the Tumor Microenvironment. Vol. 1234 31-42 (2020).
5. Hass, R. Role of MSC in the Tumor Microenvironment. *Cancers* **12**(2020).
6. Dominici, M., *et al.* Minimal criteria for defining multipotent mesenchymal stromal cells. The International Society for Cellular Therapy position statement. *Cytotherapy* **8**, 315-317 (2006).
7. Coffman, L.G., *et al.* Ovarian Carcinoma-Associated Mesenchymal Stem Cells Arise from Tissue-Specific Normal Stroma. **37**, 257-269 (2019).
8. Melzer, C., Yang, Y. & Hass, R. Interaction of MSC with tumor cells. *Cell Communication and Signaling* **14**, 20 (2016).
9. Fan, H., *et al.* Epigenetic reprogramming towards mesenchymal-epithelial transition in ovarian cancer-associated mesenchymal stem cells drives metastasis. *bioRxiv*, 2020.2002.2025.964197 (2020).
10. Goldfeld, E., Atiya, H., Frisbie, L. & Coffman, L.G. Defining the tumor cell: CA-MSC interactions which mediate ovarian cancer metastasis. *Journal of Clinical Oncology* **38**, e18072-e18072 (2020).
11. Khushman, M.d., *et al.* Exosomal Markers (CD63 and CD9) Expression Pattern Using Immunohistochemistry in Resected Malignant and Nonmalignant Pancreatic Specimens. *Pancreas* **46**, 782-788 (2017).
12. Nocquet, L., Juin, P.P. & Souazé, F. Mitochondria at Center of Exchanges between Cancer Cells and Cancer-Associated Fibroblasts during Tumor Progression. *Cancers (Basel)* **12**(2020).
13. Jackson, M.V., *et al.* Mitochondrial Transfer via Tunneling Nanotubes is an Important Mechanism by Which Mesenchymal Stem Cells Enhance Macrophage Phagocytosis in the In Vitro and In Vivo Models of ARDS. *STEM CELLS* **34**, 2210-2223 (2016).
14. Wang, X. & Gerdes, H.H. Transfer of mitochondria via tunneling nanotubes rescues apoptotic PC12 cells. *Cell Death & Differentiation* **22**, 1181-1191 (2015).
15. Herst, P.M., Dawson, R.H. & Berridge, M.V. Intercellular Communication in Tumor Biology: A Role for Mitochondrial Transfer. *Front Oncol* **8**, 344-344 (2018).
16. Au - Atiya, H.I., Au - Orellana, T.J., Au - Wield, A., Au - Frisbie, L. & Au - Coffman, L.G. An Orthotopic Mouse Model of Ovarian Cancer using Human Stroma to Promote Metastasis. *JoVE*, e62382 (2021).

17. McLean, K., *et al.* Human ovarian carcinoma–associated mesenchymal stem cells regulate cancer stem cells and tumorigenesis via altered BMP production. *The Journal of Clinical Investigation* **121**, 3206-3219 (2011).
18. Cianfanelli, F., Monlezun, L. & Coulthurst, S. Aim, Load, Fire: The Type VI Secretion System, a Bacterial Nanoweapon. *Trends in microbiology* **24**(2015).
19. Bagchi, S., Fredriksson, R. & Wallén-Mackenzie, Å. In Situ Proximity Ligation Assay (PLA). *Methods in molecular biology (Clifton, N.J.)* **1318**, 149-159 (2015).
20. Pressimone, C., Atiya, H.I., Frisbie, L. & Coffman, L. Abstract 1446: Mitochondrial transfer in the ovarian tumor microenvironment contributes to tumor stem cell phenotypes. *Cancer Research* **80**, 1446 (2020).
21. Lu, J., *et al.* Tunneling nanotubes promote intercellular mitochondria transfer followed by increased invasiveness in bladder cancer cells. *Oncotarget* **8**, 15539-15552 (2017).
22. Motohara, T., *et al.* An evolving story of the metastatic voyage of ovarian cancer cells: cellular and molecular orchestration of the adipose-rich metastatic microenvironment. *Oncogene* **38**, 2885-2898 (2019).
23. Lengyel, E. Ovarian cancer development and metastasis. *Am J Pathol* **177**, 1053-1064 (2010).